PROCEEDINGS OF SPIE

SPIEDigitalLibrary.org/conference-proceedings-of-spie

The primordial inflation polarization explorer (PIPER): current status and performance of the first flight

Samuel Pawlyk, Peter A. R. Ade, Dominic Benford, Charles L. Bennett, David T. Chuss, et al.

Samuel Pawlyk, Peter A. R. Ade, Dominic Benford, Charles L. Bennett, David T. Chuss, Rahul Datta, Jessie L. Dotson, Joseph R. Eimer, Dale J. Fixsen, Natalie N. Gandilo, Thomas M. Essinger-Hileman, Mark Halpern, Gene Hilton, Gary F. Hinshaw, Kent Irwin, Christine Jhabvala, Mark Kimball, Alan Kogut, Luke Lowe, Jeff J. McMahon, Timothy M. Miller, Paul Mirel, S. Harvey Moseley, Samelys Rodriguez, Elmer Sharp, Peter Shirron, Johannes G. Staguhn, Dan F. Sullivan, Eric R. Switzer, Peter Taraschi, Carole E. Tucker, Alexander Walts, Edward J. Wollack, "The primordial inflation polarization explorer (PIPER): current status and performance of the first flight," Proc. SPIE 10708, Millimeter, Submillimeter, and Far-Infrared Detectors and Instrumentation for Astronomy IX, 1070806 (10 July 2018); doi: 10.1117/12.2313874

SPIE.

Event: SPIE Astronomical Telescopes + Instrumentation, 2018, Austin, Texas, United States

The Primordial Inflation Polarization Explorer (PIPER): Current Status and Performance of the First Flight

Samuel Pawlyk[a,b], Peter A. R. Ade[c], Dominic Benford[b], Charles L. Bennett[a], David T. Chuss[d], Rahul Datta[b], Jessie L. Dotson[e], Joseph R. Eimer[a], Dale J. Fixsen[b,f], Natalie N. Gandilo[n,b], Thomas Essinger-Hileman[b], Mark Halpern[g], Gene Hilton[h], Gary F. Hinshaw[g], Kent Irwin[i], Christine Jhabvala[b], Mark Kimball[j], Alan Kogut[b], Luke Lowe[b,k], Jeff J. McMahon[l], Timothy M. Miller[b], Paul Mirel[b,k], S. Harvey Moseley[b], Samelys Rodriguez[b,m], Elmer Sharp III[b], Peter Shirron[j], Johannes G. Staguhn[a,b], Dan F. Sullivan[j], Eric R. Switzer[b], Peter Taraschi[b,k], Carole E. Tucker[c], Alexander Walts[a,b], and Edward J. Wollack[b]

[a]University of Maryland, College Park, USA
[b]Code 665, NASA Goddard Space Flight Center, Greenbelt, MD, USA
[c]Cardiff University, Cardiff, Wales, UK
[d]Villanova University, Villanova, PA, USA
[e]NASA Ames Research Center, Moffett Field, CA, USA
[f]University of Maryland, College Park, MD, USA
[g]University of British Columbia, Vancouver, BC, Canada
[h]National Institute for Standards and Technology, Boulder, CO, USA
[i]Stanford University, Stanford, CA, USA
[j]Code 552, NASA Goddard Space Flight Center, Greenbelt, MD, USA
[k]Wyle STE, Houston, TX, USA
[l]University of Michigan, Ann Arbor, MI, USA
[m]ADNET Systems, Inc., Bethesda, MD, USA
[n]Johns Hopkins University, Baltimore, MD, USA

ABSTRACT

The Primordial Inflation Polarization ExploreR (PIPER) is a balloon-borne instrument optimized to measure the polarization of the CMB at large angular scales. It will map 85% of the sky over a series of conventional balloon flights from the Northern and Southern hemispheres, measuring the B-mode polarization power spectrum over a range of multipoles from 2-300 covering both the reionization bump and the recombination peak, with sensitivity to measure the tensor-to-scalar ratio down to r = 0.007. PIPER will observe in four frequency bands centered at 200, 270, 350, and 600 GHz to characterize dust foregrounds. The instrument has background-limited sensitivity provided by fully cryogenic (1.7 K) optics focusing the sky signal onto kilo-pixel arrays of time-domain multiplexed Transition-Edge Sensor (TES) bolometers held at 100 mK. Polarization sensitivity and systematic control are provided by front-end Variable-delay Polarization Modulators (VPMs). PIPER had its engineering flight in October 2017 from Fort Sumner, New Mexico. This papers outlines the major components in the PIPER system discussing the conceptual design as well as specific choices made for PIPER. We also report on the results of the engineering flight, looking at the functionality of the payload systems, particularly VPM, as well as pointing out areas of improvement.

Keywords: CMB, Near Space, Balloon

Send correspondence to Samuel Pawlyk: E-mail: spawlyk@umd.edu

Millimeter, Submillimeter, and Far-Infrared Detectors and Instrumentation for Astronomy IX,
edited by Jonas Zmuidzinas, Jian-Rong Gao, Proc. of SPIE Vol. 10708, 1070806
 · doi: 10.1117/12.2313874

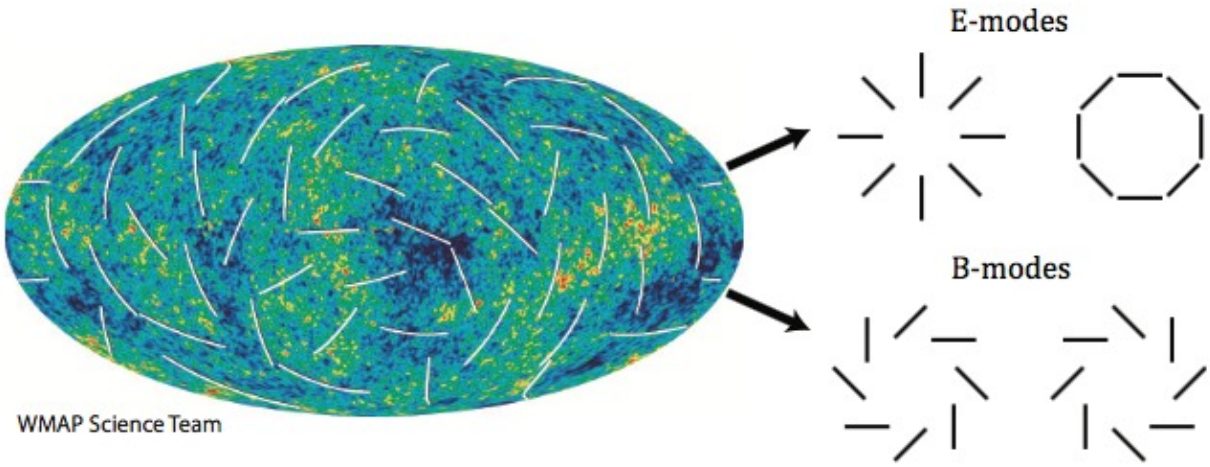

Figure 1. CMB polarization can be decomposed into two polarization types symmetric E-mode polarization and non-symmetric B-Mode polarization. Primordial B-mode polarization is caused only by tensor perturbations. In the early universe these tensors would have been caused by gravitational waves.

1. INTRODUCTION

The Cosmic Microwave Background (CMB) contains a vast amount of information about the early universe. Both the intensity of the light and the polarization contain vital clues about the origins of the universe. Polarization especially can be used to look for evidence corroborating the leading theory of cosmological development, inflation. This theory posits that shortly after the big bang the universe underwent a period of rapid expansion.[1] This inflationary period would have generated gravitational waves which would have imprinted themselves in the CMB. The CMB polarization can be broken into two parts (Fig. 1) E-mode and B-mode polarization. Scalar perturbations in the early universe such as temperature anisotropies cause only E-mode polarization. Tensor perturbations, which in the early universe would only be from gravitational waves caused by inflation, create both B-mode and E-mode polarization.[2] The level of B-mode polarization is reported as the ratio of B-modes to E-modes (r), PIPER will constrain this ratio down to r = 0.007.

The observable CMB polarization is primarily a function of two parameters, frequency and angular scale (Fig. 2). The scale of the signal refers to how large the pattern is on the sky and the age of the pattern. There are two primary 'bumps' in the pattern caused by recombination and reionization. The recombination bump occurs at a redshift of $z \approx 1000$ when the universe cools sufficiently far below the ionization threshold for atomic hydrogen to form, so that the material in the universe transitions from ionized to neutral and shows up at multipole moment $\ell \approx 180$. Reionization, which occurs at redshift $z \approx 8$ is when photons from the first stars photo-ionize hydrogen and the material of the universe transitions from neutral back to ionized, it can be seen at $\ell < 10$.[3]

Measurement of the B-mode polarization signal is complicated by foregrounds, B-modes generated after the eras of recombination and reionization. The primary foreground sources are gravitational lensing, synchrotron emission and dust (Fig. 2). Gravitational lensing is caused by dense pockets of matter that bend light transforming primordial E-modes into B-modes. Synchrotron emission is created when high energy electrons gyrate in a magnetic field.[4] By measuring multiple frequencies both near the peak CMB signal (200 GHz) and in the dust dominated frequency bands (600 GHz) PIPER will be able to clean dust foregrounds from the B-mode signal.

2. INSTRUMENT OVERVIEW

PIPER is a co-pointed twin telescope millimeter and sub-millimeter polarimeter. The payload is built up around a 3500 L dewar filled with liquid helium. The telescope is mounted inside of the dewar and the support electronics and systems are mounted to the exterior (Fig. 4). PIPER weighs approximately 5000 lbs and will fly at an altitude of 100,000 ft, above a large percentage of the atmosphere. This is advantageous as the atmosphere produces a non zero signal in the bands being measured.

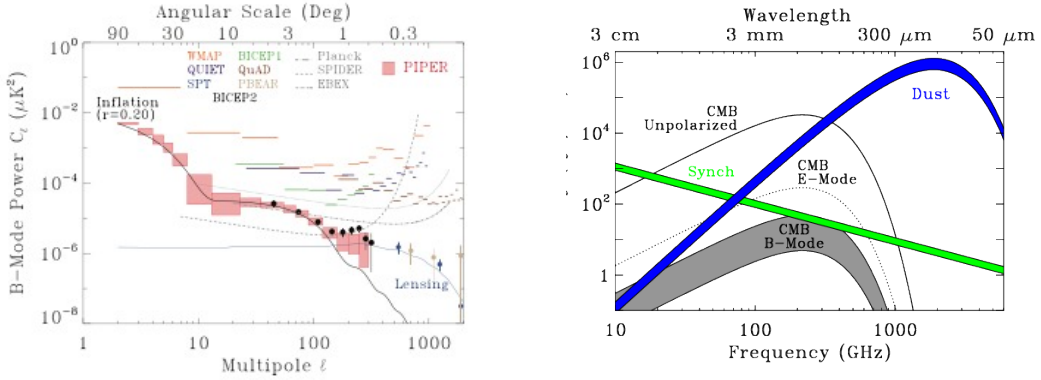

Figure 2. B-mode polarization intensity is function of both angular scale and wavelength. There are two prominent bumps in the intensity with respect to angular scale at monopoles $\ell \approx 180$ and $\ell \leqslant 10$ these are caused by recombination and reionization respectively. The polarization signal is strongest at 160 GHz however it is dominated in the foreground by both dust and synchrotron emissions at this frequency. At higher frequencies synchrotron emissions become less significant and the foregrounds can be modeled mostly by dust.

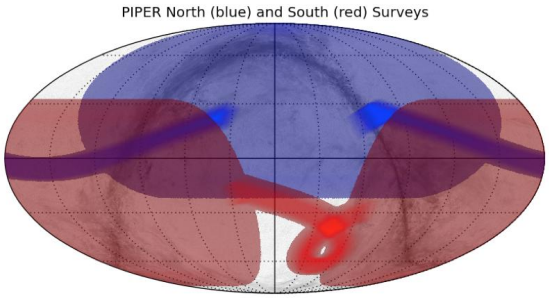

Figure 3. PIPER will fly eight traditional balloon flights, four in the northern hemisphere and four in the southern hemisphere resulting in 85% sky coverage. Each flight pair will cover a single frequency (200GHz, 270GHz, 350GHz, 600GHz). Flight data will constrain the scaler to tensor ratio r to .007 as well as creating high fidelity dust maps for ℓ from 2 to 300

The first element in PIPER's optical train is a Variable-Delay Polarization Modulator (VPM). This modulates the sky signal at 4 Hz between linear and circular polarization, with twin telescopes for Stokes Q and U. A reflective telescope illuminates an analyzer grid followed by cold stop, IR blocking filters and silicon reimaging optics. Detectors reside in a superfluid-tight submarine with silica windows, behind a final band-defining filter. A continuous adiabatic demagnetization refrigerator (CADR) maintains the transition edge bolometers at 100 mK. All optics are cooled to 1.7 K with superfluid helium pumps.

The external electronics are comprised of two Multi Channel Electronics (MCE) boxes developed by the University of British Columbia (UBC) as well as two boxes developed by the PIPER team. Each MCE handles interaction with one of the PIPER detectors. The PIPER electronic boxes are broken into "quiet" and "noisy" boxes. The noisy box contains flight computers and external sensors not related to science data collection or interpretation. The quiet box holds high speed ADCs and systems related to analysis of science data. This distinction is made to avoid contamination of the science data with multiple clocks. All inter-system communication is done using fiber optic connections.

PIPER will fly eight times and will achieve 85 percent sky coverage (Fig. 3) at four bandwidths (200, 270, 350, and 600 GHz). PIPER's night scan pattern is built around a constant speed azimuth rotation relying on the rotation of the earth to provide elevation change. During the day the pattern is similar however instead of a constant speed sweep it is an oscillating anti-solar scan. The azimuth motion is controlled using a motor with a slip clutch, the flight rotator, attaching the payload and the balloon. This system transfers momentum from the payload to balloon which due to its large size is treated as a mechanical ground. The balloon then slowly

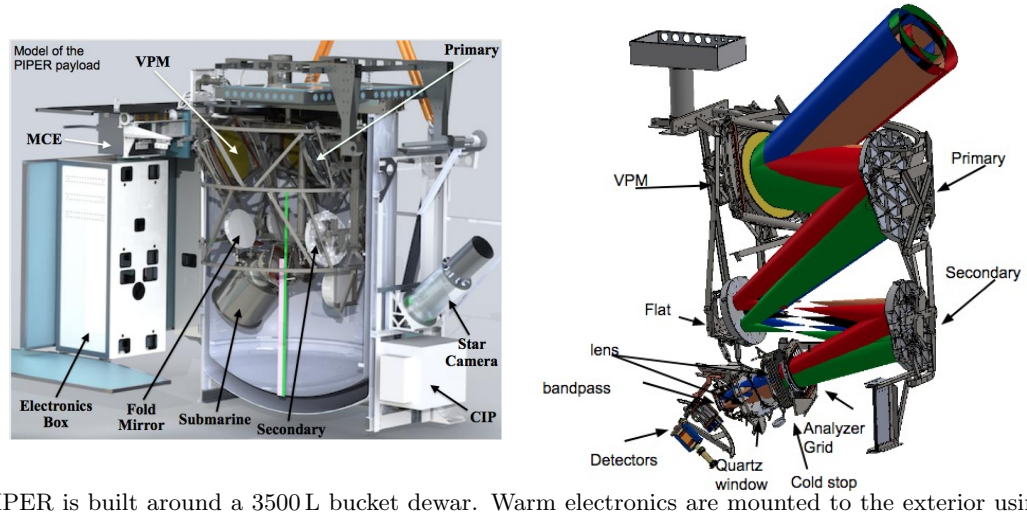

Figure 4. PIPER is built around a 3500 L bucket dewar. Warm electronics are mounted to the exterior using aluminum bracketing. Inside the dewar are co-pointed telescopes mounted to a stainless steel frame. The optical elements in order are a variable delay polarization modulator (VPM), reflective telescope, analyzer grid, cold stop, IR-blocking filters, silica window and silicon reimaging optics, all of which are kept at 1.7 K. The final element in the PIPER optical chain is a pair of transition edge sensor (TES) back-short under-grid (BUG) bolometer arrays behind a band-defining filter. An important feature of the PIPER system is that the VPM is the first optical element, the lack of a warm exterior window minimizes systematic light sources.

dumps the momentum it builds to the atmosphere through friction. Each frequency will be flown once from a northern latitude (Fort Sumner, New Mexico or Palestine, Texas) and once from Alice Springs, Australia.

3. FLIGHT PERFORMANCE

PIPER completed an engineering flight in October of 2017. The flight launched from Fort Sumner, New Mexico at 10 AM MST on October 13th, and lasted approximately 11 hours, giving a good data sample of both PIPER's day and night operational modes. This flight showed functionality of the PIPER flight systems and software. The flight also gave insight into the magnetic shielding requirements for the PIPER detectors. Data showed that the electronic systems would remain within nominal temperature ranges both during day flight and night flight. It was also demonstrated that the payload could be controlled within the required precision using the flight rotator allowing for the de-scoping of control moment gyroscopes (CMG). The VPM was also shown to to function with minimal variance in tracking using a number of different control methods. A wiring failure caused by vibration in shipment for the second campaign in Ft. Sumner disabled the fourth stage of PIPER'S CADR and resulted in the TES being held at 300 mK rather than 100 mK, leaving them normal rather than on the transition edge.

4. DETECTORS

PIPER will fly a pair of 32x40 back-short under-grid (BUG) transition-edge sensor (TES) broadband bolometer arrays.[5] Each detector array uses a single bandpass filter per flight, the filters are swapped between flights to collect data at all of the PIPER observation frequencies. The detectors are biased to 140 mK and tied to a 100 mK bath. There is a reflective back-short designed to maximize absorptivity, these are positioned behind the detectors to create resonant optical structures.[6] The absorbers and reflective back-short are (at a fixed distance) optimized for absorption in the 200 and 270 GHz science bands. The fixed distance leads to lower absorption in the 350 and 600 GHz bands. This absorption discrepancy is advantageous, since the lower absorption offsets the higher atmospheric emission at the higher frequencies, resulting in power loading at the detector that is nearly constant across the four frequency bands. The detectors are molybdenum-coated gold. They sit on the transition between normal and superconducting resistance where small energy changes create large differences in resistance. The detectors are indium bump-bonded to an array of Super-conducting Quantum Interference

Device (SQUID) time-domain multiplexers and read out using MCEs.[7] Frequency dependence is added using bandpass filters. Polarization sensitivity is added using the VPM and analyzer grid.

5. CONTINUOUS ADIABATIC DEMAGNETIZATION REFRIDGERATOR

PIPER uses a 4-stage continuous adiabatic demagnetization refrigerator (CADR) (Fig. 5) to cool its transition bolometer arrays to 100 mK. The CADR consists of four paramagnetic salts thermally connected using a series of passive and active switches (Fig. 5).[8] The stages are numbered from 1 to 4 in increasing thermal distance from the detector package. Stage 4, the largest stage, is 82 g of gadolinium-gallium garnet it can hold up to 3 A of current. The other three stages are potassium chrome alum. Stage 3 and stage 2 have identical 100 g salt pills, however stage 3 can support charges up to 4 A while stage 2 can only support 3 A. Stage 1 is 45 g and charges to 1 A.[9] Stage 4 is coupled to the helium bath via an active gas gap switch. The bath is nominally at either 4.3 K during ground testing or 1.7 K during flight usage. However due to thermal resistance between the CADR sink and the actual helium bath these numbers are closer to 4.6K and 1.8K. Stage 4 is used to cool the system to 1.2 K just above the 3-4 passive switch conduction point. Here a constant-temperature transfer is conducted between stages 4 and 3. A similar process occurs at 300 mK between stages 3 and 2. Stage 2 then cools with constant entropy below the stage 1 continuous hold point at 100 mK. Here a superconducting switch is used to tie stages 1 and 2 together while the other stages recycle. The CADR cycle can be thought of as a set of overlapping thermodynamics cycles of constant temperature and adiabatic recharges (Fig. 5). Stage 1 is an exception and maintains its temperature while cycling entropy with stage 2.

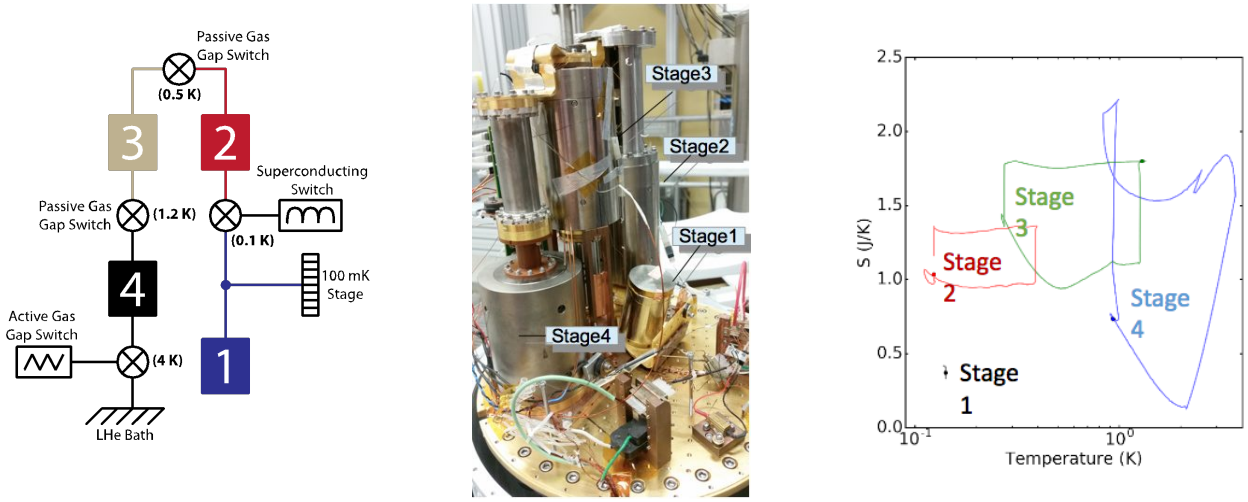

Figure 5. A four stage continuous adiabatic demagnetization refrigerator (CADR) is used to maintain PIPER's transition edge sensor (TES) bolometer arrays at 100mK. The CADR is composed of four paramagnetic salts which are connected by a series of active and passive switches to allow for heat to be dumped to the bath while holding the TESs at a constant temperature. Entropy is transfered between stages by maintaining a small temperature difference using PID control.

6. VARIABLE-DELAY POLARIZATION MODULATOR

6.1 Design

The first piece in the PIPER optics is the VPM. The VPM is composed of a movable mirror placed behind a wire grid.[10] The grid splits light into two polarized components. The wire grid has 40μm wires spaced at 114 μm.[11] Polarization parallel to the wire grid is reflected while perpendicular polarization passes through and is reflected off of the mirror and recombines with the parallel polarization (Fig. 6). The phase delay between the two linear polarizations rotates between the U and V polarizations leaving the Q polarization unchanged.[12] Equation 1 explains the relationship between U', the output U polarization, and the input U linear polarization and V circular polarization. δ is the optical phase delay. Equation 2 shows the relationship between the physical

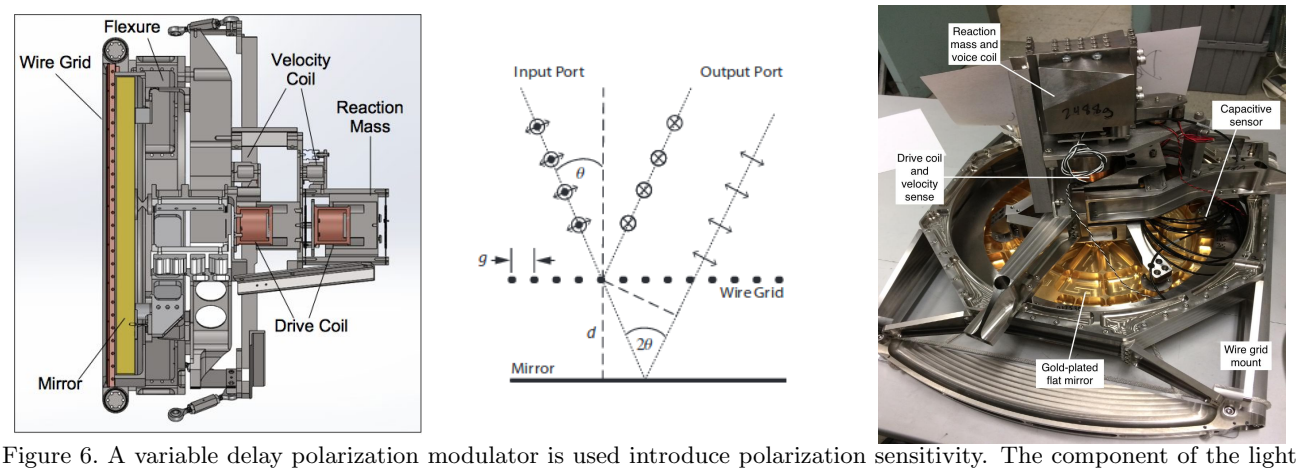

Figure 6. A variable delay polarization modulator is used introduce polarization sensitivity. The component of the light with polarization perpendicular to the wire is reflected off the grid while the parallel component passes through and reflects of the mirror. This introduces a phase delay which is linearly dependent on the distance between the wire gird and mirror. PIPER uses voice coils to move the mirror in a sinusoidal pattern to achieve the desired variable phase delay. A secondary reaction mass is used to null momentum from the mirror and minimize payload shaking which could introduce systematic B-mode polarization

distance d and the the phase delay δ. This relation assumes that the wavelength is much larger than length scales of the grid geometry. θ is the incident angle of the light with respect to the wire grid (Fig. 6).

$$U' = U\cos\delta + V\sin\delta \tag{1}$$

$$\delta = \frac{4\pi d}{\lambda}\cos\theta \tag{2}$$

The PIPER VPM (Fig. 6) has two movable pieces, a main mirror and a reaction mass designed to null vibration. The reaction mass is half the mass of the mirror and therefore must be run 180 degrees out of phase and with twice the amplitude of the mirror to null the combined momentum. The mirror and reaction mass are mounted on flexure's and controlled by voice coils. The mirror has three capacitive sensors that are used to get position measurements for control and data recreation as well as to ensure that the mirror does not twist. The reaction mass has only one capacitive sensor as flatness is not a concern here. Both the mirror and reaction mass have a secondary voice coil that is used to collect velocity measurements, used for PID control.

6.2 Flight Performance

In flight, PIPER's VPM was run using three different control modes. This was done in response to issues that appeared in ground testing once the telescope was taken to cryogenic temperatures. Because of the size of the mirrors, cryogenic testing of the systems was not possible outside of the flight dewar and was left to pre-flight field testing. PIPER's three run modes are a PID control loop, a PI control loop and an open loop run mode. The PI mode eliminates the velocity sensor as an input and therefore removes feedback issues caused by it. The open loop mode outputs a set power and therefore removes the risk of control loop instability altogether. Figures 7 and 8 show the flight behavior of the VPM. Measurements were made at 50 Hz. The primary requirement of the VPM is the ability to hit a desired throw range. The desired throw for the VPM to maximize circular polarization response, the goal for the engineering flight, is from -140 μm to 535 μm as measured with the capacitive sensor used for mirror control. It is easy to see in the left most plot of Fig. 7 that only the two PID modes, which lie directly on top of each other, achieve this goal. The open loop control comes close. **The system dynamics are not well characterized. This means that open loop runs must be tuned by eye. PI control also has issues it does not handle desired trajectories that are not centered about the zero point well. The PI control strategy also requires the commanded amplitude to be slowly ramped up to avoid instability. It is import that the capacitive sensors have the ability to accurately recreate VPM position after flight in order to correctly model the polarization. Decreasing the RMS between**

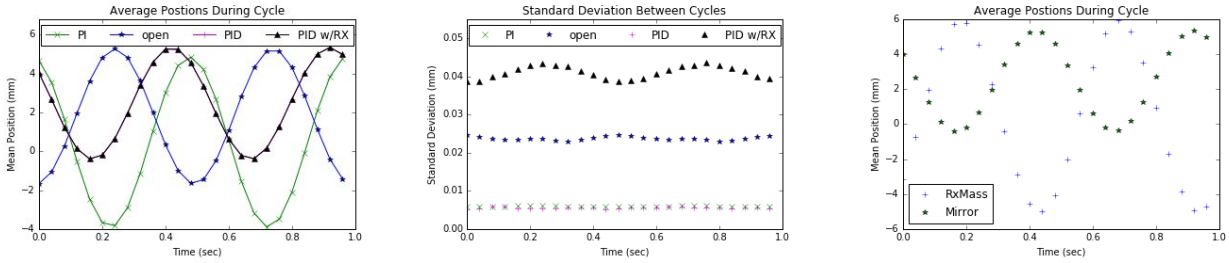

Figure 7. (Left) The mean position of the VPM over over a one second interval, it is an average of 100 s of seconds. The four lines show four different control modes. (Center) The standard deviation of each measurement point in the cycle during the same period. (Right) The mean of the VPM and reaction mass while both were controlled simultaneously using a PID.

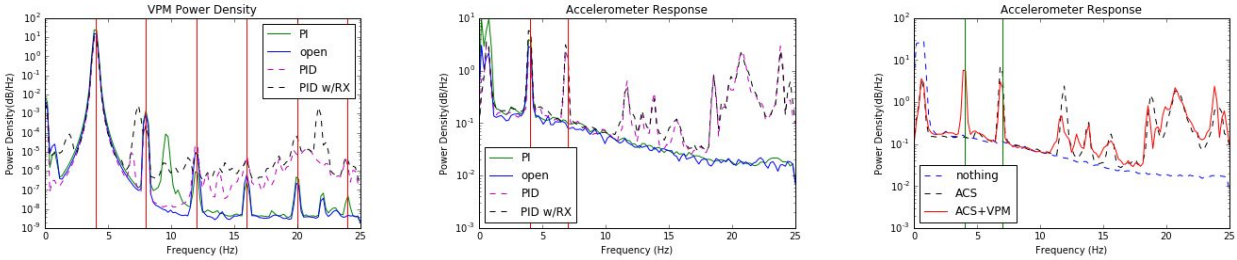

Figure 8. The frequency response of the PIPER telescope is an important measure of camera stability. Un-modeled vibration can introduce systematic B-mode signals into measurements. There are two primary causes of vibration in the PIPER system, the VPM and the CMGs. The VPM oscillates at a frequency of 4Hz, the CMG rotate nominally at 7Hz. The VPM only creates frequency spikes at 4Hz and its higher harmonics. These spikes don't show up in the accelerometer due to the higher noise floor. The CMG creates a frequency spike at 7Hz and also at higher frequencies which alias into the measurement (Right). VPM Fourier transform (Left) is calculated from using a capacitive sensor measuring VPM position. The accelerometer transform (Center, Right) is calculated using accelerometers mounted with the warm electronics on the outside of the payload

cycles will lead to better position reconstruction. Here the center plot of Fig. 7 is examined. It can be seen that the lowest deviations are found using the PID and PI control algorithms when the reaction mass is not running. The open loop has deviations at approximately two times the others. The reaction mass brings this number up to four times the minimum and adds a dependency on where in the sine wave the mirror is. Looking at the right most plot the reason for this is clear. The track of the mirror and reaction mass should be exactly out of phase however they are slightly offset.

Another way to examine the performance of the VPM is through the frequency response both of the VPM and the entire payload (Fig. 8). The left most plot shows a Fourier transform of the VPM position as measured by the capacitive sensors. In the VPM data there are clear frequency spikes at 4 Hz as well as at higher harmonics. The center plot shows a Fourier transform of the PIPER payload accelerometer. Here peaks can be seen at 4Hz and 7 Hz, the 4 Hz signal is from the VPM the 7Hz signal is from PIPERS CMG wheels which were run at that frequency. The higher harmonics of the VPM do not show up in the accelerometer data because the vibration floor (10^{-1} dB/Hz to 10^{-2} dB/Hz) is well above the level of the higher harmonics (10^{-3} dB/Hz to 10^{-8} dB/Hz.)

All of the control modes do a good job of only exciting modes at 4 Hz and higher harmonics. While using the PID mode, there is clear aliasing of high frequency signals. This noise only appears when the CMG is running and is not increased by the VPM. The CMG has been descoped and therefore it is not considered an issue. The VPM meets its functional requirements and also offers contingency modes which can resolve unexpected stability issues.

7. THERMAL SYSTEMS

An important design feature of the PIPER payload is the cryogenic optics. Keeping the forward mirrors below the temperature of the measured signal (2.725 K) minimizes light emission and leads to background limited measurements. An examination of all of the internal temperatures (Fig. 9) shows that as long as the super-fluid pumps are functioning properly, all of the forward optics can be held at the bath temperature of 1.7 K. For simplicity the pumps were run at maximum power during the flight. The combined power dissipation to the LHe bath was around 100W and was desirable to ensure a steady flow of helium gas. It was also demonstrated that helium flow can be maintained and the optics kept cold using only 25% of pump capacity. This would be advantageous during longer-duration flights where running out of helium becomes a concern.

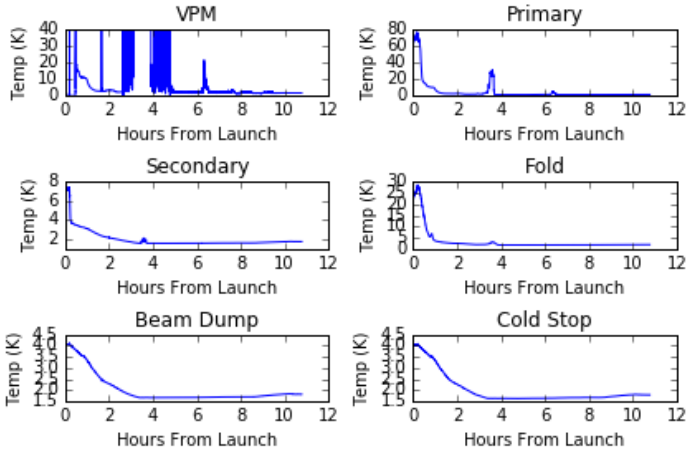

Figure 9. An important feature of the PIPER measurement scheme is cryogenic forward optics. Once the payload had reached altitude PIPER is able to keep all of it optical elements at 1.7 K using a series of super-fluid pumps. The temperatures only spiked when power was not applied to one or more of the pumps.

8. ELECTRONIC SYSTEMS

PIPER's flight electronics are built around dsPIC30F5011 chips. The primary consideration behind this design choice is the need minimize the number of clocks to avoid aliasing slow beat frequencies. To this end, the flight electronics all run off a common external clock. During flight this external clock is provided by the MCE sync box. The boards are grouped into backplanes with each containing a master control board (PMaster) which handles distribution of the sync-box clock and interaction with flight computer. Commands are passed along a common channel to all boards. Each sub-board is given an address between zero and sixteen which allows it to react only to commands directed at it. The address also gives the board a defined "talk" slot. This slot is the portion of a 1 Hz frame where the board outputs data packets, this sectioning avoids boards talking over each-other.

Outside of the PMaster board, PIPER has five slave boards and a pseudo-slave board. These boards are a PID control board (DSPID), a sensitive 4-wire measurement board (TREAD), a board designed for driving 3-phase motors (PMotor), an analog measurement board (AnalogIn) and an analog control board (AnalogOut). These boards all share power, clock and data signals with the Pmaster. The pseudo-slave board is a high speed analog measurement board (PsyncADC). It only shares power and clock but has its own data lines to facilitate high volume data transfer.

The DSPID board is the control board for PIPER's CADR. Each stage of the CADR has a DSPID board controlling it. The board is built around an analog to digital converter (ADC) and a digital to analog converter (DAC). The board handles PID control of the stage temperature and current levels, and constant current changes. One important feature of this board is that due to memory constraints and the desire to have the boards be interchangeable, the PID is done in resistance space rather than temperature space. Since the $\Omega - K$ curve is

not linear, this means that PID control loops must be tuned individually not only for each stage but also for each temperature range.

The Tread board makes 4-wire measurements of PIPER's cryogenic thermometers and Hall probes. The board has three separate modes to accommodate different sensor types a diode measurement mode a ruthenium oxide measurement mode and a low resistance measurement mode which is used to read Hall probes. The board measures up to 16 channels at 1 Hz.

PMotor is PIPER's second PID control board. It was originally designed to drive 3-phase motors for the attitude control system. With alternate firmware, it is also used to control the VPM voice coils. The board is comprised of two 16-bit four channel DACs and an ADC with an eight channel multiplexer. Unlike the rest of the PIPER electronics the PMotor board is built around the dsPIC30F5015. This change was made to gain access to the quadrature encoder functionality necessary to interact with the chosen three-phase motors. In the motor driving configuration the DAC uses three of its channels to generate the characteristic three-phase signal and the fourth channel as a linear scale to control motor speed. The ADC is used to measure current levels and read out absolute position sensors where necessary. In the VPM driving configuration one board is used for each driving coil (mirror and reaction mass). One channel of the DAC is used to output a driving signal to the primary voice coil. The ADC is used to collect position and velocity measurement data from a capacitive sensor and a secondary voice coil. The measurements are made concurrently rather than simultaneously. However the control algorithm assumes simultaneous measurements at 2 kHz.

The AnalogIn and AnalogOut boards are used to measure warm "payload thermometers" and control survival heaters and other non-precision systems. Both the AnalogIn and AnalogOut boards have 32 channels and measure/update at 1 Hz.

The final board is the psyncADC or fast ADC board. This board is used to make measurements of systems where high speed data is required for post-flight analysis. This board has 32 channels and is used to take measurements of the VPM positions as well as measurements of PIPER's pointing sensors (gyroscopes, magnetometers, clinometers and accelerometers).

9. FLIGHT SOFTWARE

PIPER's software systems run on four Intel Atom based low-power computers that run Ubuntu 14.01. PIPER has a primary flight computer that handles interaction with the ground station as well as control of PIPER bus electronics. It has two secondary computers for detector interaction, one for each of the MCEs. It also has a dedicated computer for control of its star camera. Inter computer interaction is handled via Ethernet protocol with static IP addresses allowing for easy connection of ground station electronics.

PIPER's process management is handled by Ubuntu's upstart daemon capabilities. This ensures that unless the operating system has a fatal lockup systems can be started and run independently. The PIPER flight software relies on a publish-subscriber model to handle inter process communication, and is built around the Redis database. Each process is single-threaded and has a single task. Figure 10 shows the conceptual design of the PIPER flight software system.

PIPER's flight plan is based around semi-autonomously operation with data stored on-board and recovered post-flight when the payload is retrieved. The software is designed with an end goal of having a very low command rate, only requiring human interaction to change between observation modes. However all the systems with the exception of the CADR, which requires fast and well-coordinated inputs, can fall back to manual control. There are two distinct command types, discrete and data word. Discrete commands are not interpreted by the PIPER software and are used used for gondola power control. The data word commands are 16-bits long and must be defined prior to flight. PIPER splits the command space using the first 8-bits as "addresses", which give the command type, and the second 8-bits for required argument values. PIPER uses a web-based graphical interface on the ground to translate from human understandable commands into the 16-bit commands. While all data is stored on-board and the nominal science plan is to retrieve the hard drives post-flight PIPER also continuously down-links a down-sampled set of its housekeeping data. This is done for two reasons. The primary reason is to allow the flight operators to monitor functionality and give the capability to switch to manual control if necessary. The down-link also offers some contingency if the payload is not recoverable after the flight. The

science data is not continuously down-linked, as the file sizes are too large, but the option exists for down-links of single datasets.

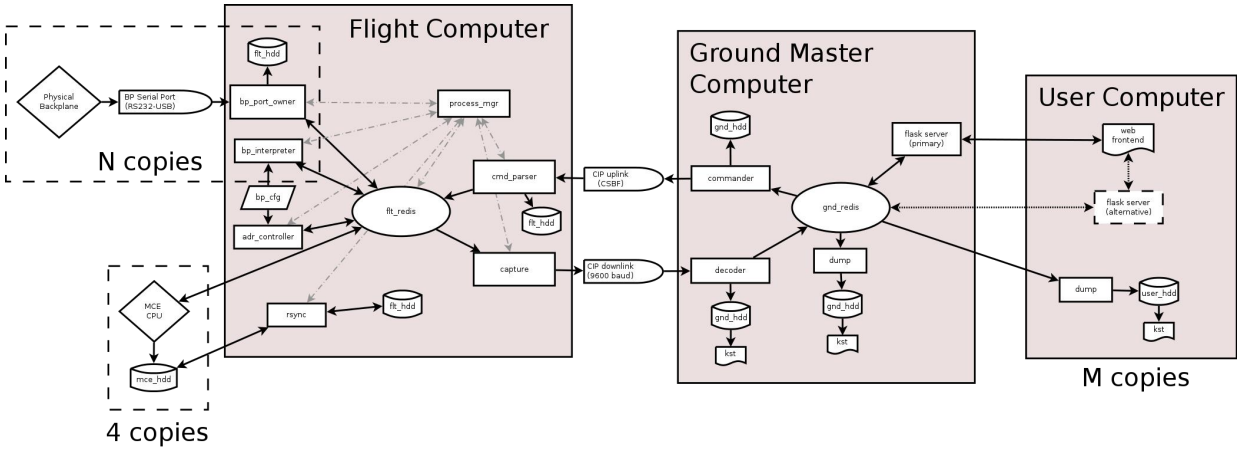

Figure 10. PIPER software is built around a distributed pub-sub architecture. The open-source software package Redis is used to handle pub-sub communication. The responsibility of each processes is minimized to allow for code reuse, configuration files hold specific information required to complete tasks.

10. CONCLUSION

The PIPER mission will provide measurements of both the B-mode polarization in the CMB and of dust foregrounds. The large angular scales and multiple frequency bands will contribute crucial data to the CMB community and be able to constrain the scaler to tensor ratio to $r = 0.007$. In October of 2017 PIPER had a successful engineering flight demonstrating functionality of its bus systems and ability to survive landing without catastrophic damage. Based on the results of this flight PIPER will launch the first of its eight science flights in June of 2018.

REFERENCES

[1] Davis, R. L., Hodges, H. M., Smoot, G. F., Steinhardt, P. J., and Turner, M. S., "Cosmic microwave background probes models of inflation," *Phys. Rev. Lett.* **69**, 1856–1859 (Sep 1992).

[2] Hu, W. and White, M. J., "A CMB polarization primer," *New Astron.* **2**, 323 (1997).

[3] Mortonson, M. J., Dvorkin, C., Peiris, H. V., and Hu, W., "CMB polarization features from inflation versus reionization," *Phys. Rev.* **D79**, 103519 (2009).

[4] Smoot, G. F., "Synchrotron Radiation as CMB Foreground," *ArXiv Astrophysics e-prints* (Feb. 1999).

[5] Jhabvala;, C. A., "Kilopixel backshort-under-grid arrays for the primordial inflation polarization explorer," *Society of Photographic Instrumentation Engineers* **9153**, 127 (2014).

[6] Miller, T. M., "Infrared-bolometer arrays with reflective backshorts," Tech. Rep. GSC-15104-1, Goddard Space Flight Center, Greenbelt, MD, United States (April 2011).

[7] Battistelli, E. S., Amiri, M., Burger, B., Halpern, M., Knotek, S., Ellis, M., Gao, X., Kelly, D., Macintosh, M., Irwin, K., and Reintsema, C., "Functional Description of Read-out Electronics for Time-Domain Multiplexed Bolometers for Millimeter and Sub-millimeter Astronomy," *Journal of Low Temperature Physics* **151**, 908–914 (May 2008).

[8] Shirron, P. J., Canavan, E. R., DiPirro, M. J., Tuttle, J. G., and Yeager, C. J., [*A Multi-Stage Continuous-Duty Adiabatic Demagnetization Refrigerator*], 1629–1638, Springer US, Boston, MA (2000).

[9] Kimball, M. O., "Piper continuous adiabatic demagnetization refrigerator," Space Cryogenics Workshop 2017 (2017).

[10] Chuss, D. T., Wollack, E. J., Moseley, S. H., and Novak, G., "Interferometric polarization control," *Appl. Opt.* **45**, 5107–5117 (Jul 2006).

[11] Chuss, D. T., Eimer, J. R., Fixsen, D. J., Hinderks, J., Kogut, A. J., Lazear, J., Mirel, P., Switzer, E., Voellmer, G. M., and Wollack, E. J., "Variable-delay polarization modulators for cryogenic millimeter-wave applications," *Review of Scientific Instruments* **85**, 064501 (June 2014).

[12] Chuss, D. T., Wollack, E. J., Henry, R., Hui, H., Juarez, A. J., Krejny, M., Moseley, S. H., and Novak, G., "Properties of a variable-delay polarization modulator," *Appl. Opt.* **51**, 197–208 (Jan 2012).